AIP | Journal of Applied Physics

Analysis and design of terahertz antennas based on plasmonic resonant graphene sheets

M. Tamagnone, J. S. Gómez-Díaz, J. R. Mosig, and J. Perruisseau-Carrier

Citation: J. Appl. Phys. **112**, 114915 (2012); doi: 10.1063/1.4768840
View online: http://dx.doi.org/10.1063/1.4768840
View Table of Contents: http://jap.aip.org/resource/1/JAPIAU/v112/i11
Published by the American Institute of Physics.

Analysis and design of terahertz antennas based on plasmonic resonant graphene sheets

M. Tamagnone,[1,2] J. S. Gómez-Díaz,[1] J. R. Mosig,[2] and J. Perruisseau-Carrier[1,a)]
[1]*Adaptive MicroNano Wave Systems, LEMA/Nanolab, Ecole Polytechnique Fédérale de Lausanne (EPFL), 1015 Lausanne, Switzerland*
[2]*Laboratory of Electromagnetics and Acoustics (LEMA), Ecole Polytechnique Fédérale de Lausanne (EPFL), 1015 Lausanne, Switzerland*

(Received 19 September 2012; accepted 7 November 2012; published online 14 December 2012)

Resonant graphene antennas used as true interfaces between terahertz (THz) space waves and a source/detector are presented. It is shown that in addition to the high miniaturization related to the plasmonic nature of the resonance, graphene-based THz antenna favorably compare with typical metal implementations in terms of return loss and radiation efficiency. Graphene antennas will contribute to the development of miniature, efficient, and potentially transparent all-graphene THz transceivers for emerging communication and sensing application. © *2012 American Institute of Physics*. [http://dx.doi.org/10.1063/1.4768840]

I. INTRODUCTION

The last decade has witnessed growing interest in graphene and its potential applications in various fields,[1] including active electromagnetic devices.[2] However, only few initial works considered the use of graphene in antennas and other passive devices.[3–6] This is especially true for antenna applications, where graphene was first considered as a parasitic layer below a dipole antenna made of gold and radiating at millimeter-wave frequencies (120 GHz).[7] Thus, graphene itself was not supporting radiation there; in fact, it was placed in close proximity to the gold dipole to selectively allow or prevent radiation through graphene electric field biasing, which could as well be simply achieved in the front-end. Second, the scattering of an incident wave impinging on graphene rectangular patches was studied.[8] There it was confirmed that the graphene patches support surface plasmon resonances in the terahertz (THz) range, and the resonant frequencies were successfully correlated with a theoretical plasmon wavelength for an infinite sheet previously derived in Refs. 9 and 10.

In this letter, we present the first study—to the authors' knowledge—on graphene used as an actual antenna radiator, namely, *as an electromagnetic interface between free-space and a receiver/transmitter*. Indeed, the majority of graphene-integrated THz sensor or emitter applications require the coupling of a free-space wave to a THz detector or source (e.g., a photomixer). In this case, parameters such as the input impedance and the radiation efficiency, which have not been studied so far, are the most important to evaluate if proper emission/reception can be achieved. Here, it is shown that well-designed and excited graphene antennas can be optimized for high input impedance, as needed for matching to, e.g., THz photomixers, and that satisfactory efficiency can be obtained despite the very high operation frequency and plasmon-induced very small electrical size of the antenna.

Finally, an additional incentive for the development of graphene THz antennas is the integration of graphene-only transceivers. Indeed, graphene is an extremely promising material for ultra-high frequency analog circuits as well,[11] and THz is currently attracting tremendous interest in both sensing and communication[12] applications. Such transceivers could be integrated in transparent and flexible screens.[1,11]

II. TM SURFACE PLASMON-POLARITON (SPP) MODE IN GRAPHENE

In this section, the plasmon propagation on graphene is computed for both infinite and finite-width graphene strips using a full-wave solver (Ansys HFSS). This allows, respectively, to (i) rigorously verify that the used solver correctly models the unusual and dispersive graphene conductivity, thereby validating the presented antenna simulations, and (ii) relate antenna parameters to the corresponding plasmon wavelength for finite-width antennas surrounded by arbitrary dielectrics.

Thanks to its ultra-thin electrical thickness, graphene can be rigorously modeled by a surface conductivity σ.[8–10] Its value is determined by Kubo's formula,[10] which expresses the dependence of σ on temperature T, scattering rate $\Gamma = 1/(2\tau)$, where τ is the transport relaxation time, chemical potential μ_c and frequency ω. Throughout this work, the following parameters are considered: T = 300 K, $\tau = 1$ ps (typical value[3,10]), μ_c up to 0.25 eV. Here Kubo's formula is approximated considering only the intraband contribution[10]

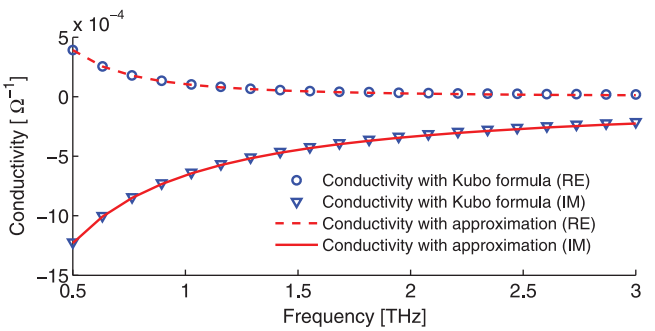

FIG. 1. Comparison between the complete Kubo's formula and its approximation 1 with $\mu_c = 0$ eV (worst case).

a)Electronic mail: julien.perruisseau-carrier@epfl.ch.

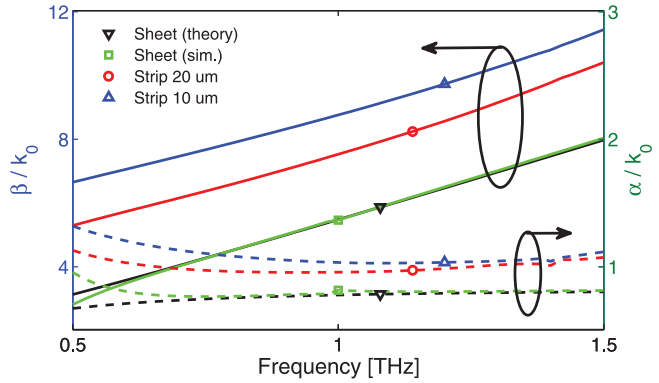

FIG. 2. Comparison between k on: infinite sheet (theoretical and simulation), 5 and 10 μm strip (simulation).

$$\sigma(\omega,\mu_c,\Gamma,T) \approx -j\frac{q_e^2 k_B T}{\pi\hbar^2(\omega - j2\Gamma)} \times \left(\frac{\mu_c}{k_B T} + 2\ln(e^{-\mu_c/(k_B T)} + 1)\right). \quad (1)$$

A comparison between complete Kubo's formula and 1 (see Fig. 1) demonstrates the accuracy of this approximation for the considered parameters.

It is well-known that the inductive nature of σ seen in Fig. 1 allows an infinite graphene sheet to support TM surface waves, also referred to as SPP, since the conductivity results from the plasma-like behavior of the electrons.[10] In the case of an *infinite* layer sandwiched between two dielectrics, the dispersion relation of the mode is given by[9]

$$\frac{\epsilon_{r1}}{\sqrt{k^2 - \epsilon_{r1}k_0^2}} + \frac{\epsilon_{r2}}{\sqrt{k^2 - \epsilon_{r2}k_0^2}} = \frac{-j\sigma}{\omega\epsilon_0}, \quad (2)$$

where $k = \beta - j\alpha$ is the guided complex propagation constant, $k_0 = \omega/c$ is the free space wavenumber, β is the guided wave number, α is the propagation attenuation, and c is the speed of light in vacuum.

Though any—and potentially multilayer—substrate can be handled by the full-wave approach used here, in this work, we consider a transparent glass substrate, which exhibits a permittivity $\epsilon_r = 3.8$ and negligible losses at THz.[13] The corresponding simulation of the plasmonic mode supported by an infinite sheet can be achieved exploiting the nature of the TM mode. Notably, two parallel H-symmetry boundary planes are placed on the sides of a graphene rectangle to create a finite equivalent model. Waveports are used to excite the structure, and the propagation constant k of the mode is retrieved using standard transmission line techniques. Fig. 2 clearly shows the excellent agreement between 2 and the full-wave retrieved results, validating the simulation of the graphene conductivity.

TABLE I. Proposed antennas and corresponding W.P. The last column shows the electrical length with respect to the free space wavelength.

Antenna	μ_c (eV)	L (μm)	W (μm)	W.P.	f (THz)	Z_{in} (Ω)	L/λ_0
1	0.13	17	10	L	1.023	77	0.06
				H	1.35	1020	0.08
2	0.25	23	20	L	1.172	33	0.09
				H	1.534	425	0.12

As a further step towards the antenna design, the SPP mode has been simulated also on finite width strips for which no analytical formula is available. Note that the size of the strips considered here is large enough to neglect non-local quantum effects.[14] The simulation has been performed for several values of the strip width (Fig. 2). Importantly, narrower strips are characterized by larger β, namely "slowing" the mode, which is related to the confinement of moving charges, hence more inductive behavior.

III. THz ANTENNAS BASED ON GRAPHENE

A rectangular W × L graphene patch can be regarded as a finite length L strip with width W. Since the SPP mode can propagate on finite-width strips, the patch is expected to support standing wave resonances approximately (due to fringing fields) given by $L = n\lambda/2 = n\pi/\beta$, where β is the wave number of the finite-width strip plasmon previously computed. This work focuses on the first resonance ($n = 1$) for smallest size and best-behaved input impedances. The length of the antenna is selected using the resonance condition and considering a target resonance frequency of 1 THz.

As mentioned in the Introduction, we aim here at designing actual antennas acting as interfaces between free space propagation and a lumped source/detector, rather than simple scatterers. Radiation is achieved placing a THz continuous-wave (CW) photomixer in the middle of the patch (see Fig. 3(a)). In transmission (see Figs. 3(b) and 3(c)), the photomixer excites the patch resonance which

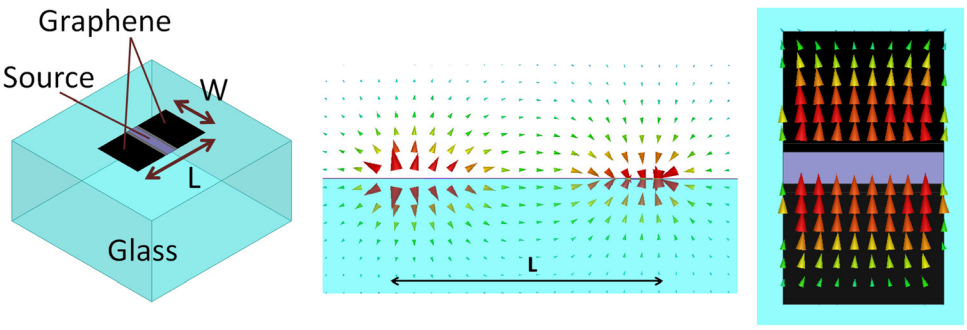

(a) (b) (c)

FIG. 3. (a) Graphene-sheet resonant plasmon antenna. (b) Electric near field distribution. (c) Surface current density.

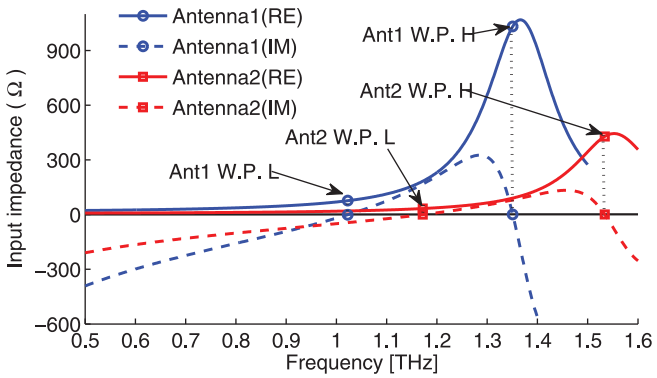

FIG. 4. Input impedance Z_{in} of the proposed antennas. The arrows indicate the real impedance W.P.

enables radiation (note that a DC bias must be applied between both graphene half-sections here). Reciprocally, in reception, the incident power is delivered to the photomixer that can operate also as a detector.

Different antennas were designed using the strip plasmon mode simulation approach shown in Sec. II, assuming different chemical potentials μ_c. Table I shows the corresponding antenna dimensions for two representative examples, hereafter referred to as antennas 1 and 2, respectively.

The input impedance Z_{in} of the antennas is shown in Fig. 4. Each antenna shows two frequency working points (W.P.) where Z_{in} is real: the first one (referred to as L) with a low resistance value, the second one (H) with a high value. The latter is particularly interesting since THz photomixers generally show a very high and real output impedance.[15,16] It is noticeable that placing the source in an asymmetric position (closer to one extremity than the other) provides an additional degree of freedom for Z_{in}. However, this leads in general to lower Z_{in}.

Fig. 5(a) shows that higher μ_c values lead to larger radiation efficiencies η_r. This effect is mainly due to the larger resonating size of the antenna for higher μ_c. Avoiding excessively small values for W is also important to maximize η_r. Fig. 5(b) shows the total efficiency $\eta_m\eta_r$ where η_m is the impedance matching efficiency. η_m is computed using a realistic value of 10 kΩ for the photomixer impedance. The observed efficiencies are low compared to antennas operating at microwave and millimeter wave frequency, but are actually better as compared with typical THz antennas[16]—where η_m alone is less than 1% for a 10 kΩ photomixer—and despite the miniaturized size of the proposed antennas.

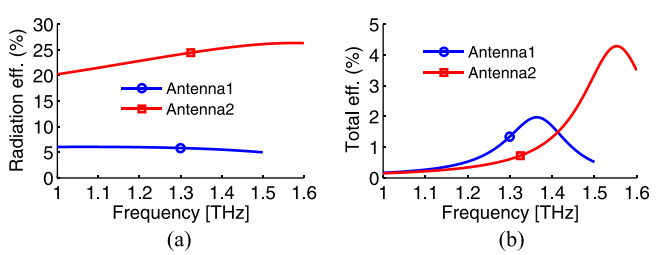

FIG. 5. (a) Radiation efficiency η_r. (b) Total efficiency $\eta_m\eta_r$ assuming a 10 kΩ photomixer.

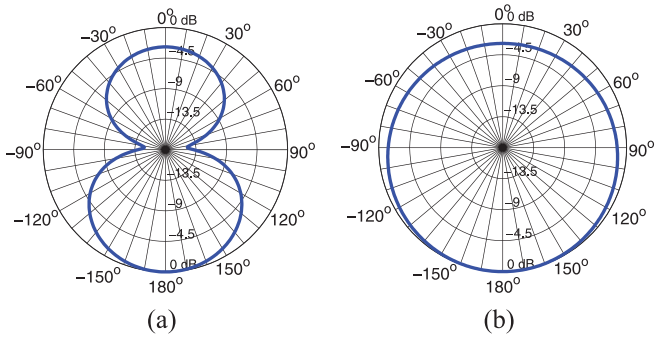

FIG. 6. Radiation pattern (antenna 1, W.P. H.) (a) E-plane, (b) H-plane. Cross polarization is zero by symmetry.

The radiation patterns in Fig. 6 resemble those of conventional (non-plasmonic) short dipoles. This is expected for such miniaturized antennas, since the current density is concentrated in the antenna phase center, leading to a radiation similar to the hertzian dipole. The THz radiation is mostly directed in the substrate direction, which is desired in case a dielectric lens is used to improve directivity.[15] It was also verified that adding such a lens has a negligible impact on the input impedance.

IV. CONCLUSION

It has been shown that graphene is a promising material for the realization of miniaturized resonant THz antennas. Good direct matching can be achieved to THz CW photomixers even with simple geometries. The radiation efficiency is good given the extremely small electrical size, leading to performances comparable to or better than metal implementations. These results are especially interesting in the light of recent very promising developments in high-frequency analog actives[2,11] and sources[17–19] based on graphene, paving the way to the future integration of the whole THz front end on graphene. Finally, it is worth mentioning that the presented concept can be extended to enable dynamic reconfiguration via graphene's field effect.[20]

ACKNOWLEDGMENTS

This work was supported by the Hasler Foundation, Project 11149, by the Swiss National Science Foundation (SNSF) under Grant No. 133583, and by the EU FP7 Marie-Curie IEF Grant No. 300966. Discussion on THz photomixers with Professor Y. Huang is appreciated.

[1]K. Geim and K. S. Novoselov, Nature Mater. **6**, 183 (2007).
[2]F. Schwierz, Nat. Nanotechnol. **5**, 487 (2010).
[3]A. Vakil and N. Engheta, Science **332**, 1291 (2011).
[4]P. Y. Chen and A. Alù, in *2012 IEEE Antennas and Propagation Symposium*, Chicago, Illinois, USA, 8–14 July 2012 (IEEE, 2012), p. if53.7.
[5]J. S. Gómez-Díaz, J. Perruisseau-Carrier, P. Sharma, and A. Ionescu, J. Appl. Phys. **111**, 114908 (2012).
[6]H. S. Skulason, H. V. Nguyen, A. Guermoune, V. Sridharan, M. Siaj, C. Caloz, and T. Szkopek, Appl. Phys. Lett. **99**, 153504 (2011).
[7]M. Dragoman, A. A. Muller, D. Dragoman, F. Coccetti, and R. Plana, J. Appl. Phys. **107**, 104313 (2010).
[8]I. Llatser, C. Kremers, D. N. Chigrin, J. M. Jornet, M. C. Lemme, A. Cabellos-Aparicio, and E. Alarcon, in *6th European Conference on*

Antennas and Propagation, Prague, Czech Republic, 26–30 March 2012 (IEEE, 2012), pp. 194–198.
[9]M. Jablan, H. Buljan, and M. Soljacic, Phys. Rev. B **80**, 245435 (2009).
[10]G. W. Hanson, J. Appl. Phys. **103**, 064302 (2008).
[11]P. Avouris, Nano Lett. **10**, 4285 (2010).
[12]M. Tonuochi, Nat. Photonics **1**, 97 (2007).
[13]M. Naftaly and R. E. Miles, Proc. IEEE **95**, 1658 (2007).
[14]J. Christensen, A. Manjavacas, S. Thongrattanasiri, F. H. L. Koppens, and F. J. García de Abajo, ACS Nano **6**, 431 (2012).
[15]I. S. Gregory, C. Baker, W. R. Tribe, I. V. Bradley, M. J. Evans, E. H. Linfield, A. G. Davies, and M. Missous, IEEE J. Quantum Electron. **41**, 717 (2005).
[16]Y. Huang, N. Khiabani, Y. Shen, and D. LI, in *International Workshop on Antenna Technology (iWAT), Kowloon, Hong Kong, March 7–9, 2011* (IEEE, 2011), pp. 152–156.
[17]F. Rana, IEEE Trans. Nanotechnol. **7**, 91 (2008).
[18]A. Satou, F. T. Vasko, T. Otsuji, and V. Ryzhii, in *International Conference on Simulation of Semiconductor Processes and Devices*, San Diego, California, USA, 9–11 September 2009 (IEEE, 2009), pp. 261–264.
[19]V. Ryzhii, M. Ryzhii, V. Mitin, and T. Otsuji, J. Appl. Phys. **110**, 094503 (2011).
[20]M. Tamagnone, J. S. Gómez-Díaz, J. R. Mosig, and J. Perruisseau-Carrier, Appl. Phys. Lett. **101**, 214102 (2012).